Targeted Loss of GHR Signaling in Mouse Skeletal Muscle Protects Against High-Fat Diet–Induced Metabolic Deterioration

Archana Vijayakumar,[1] YingJie Wu,[1] Hui Sun,[1] Xiaosong Li,[2] Zuha Jeddy,[1] Chengyu Liu,[3] Gary J. Schwartz,[2] Shoshana Yakar,[1] and Derek LeRoith[1]

Growth hormone (GH) exerts diverse tissue-specific metabolic effects that are not revealed by global alteration of GH action. To study the direct metabolic effects of GH in the muscle, we specifically inactivated the growth hormone receptor *(ghr)* gene in postnatal mouse skeletal muscle using the Cre/loxP system (mGHRKO model). The metabolic state of the mGHRKO mice was characterized under lean and obese states. High-fat diet feeding in the mGHRKO mice was associated with reduced adiposity, improved insulin sensitivity, lower systemic inflammation, decreased muscle and hepatic triglyceride content, and greater energy expenditure compared with control mice. The obese mGHRKO mice also had an increased respiratory exchange ratio, suggesting increased carbohydrate utilization. GH-regulated suppressor of cytokine signaling-2 *(socs2)* expression was decreased in obese mGHRKO mice. Interestingly, muscles of both lean and obese mGHRKO mice demonstrated a higher *interleukin-15* and lower *myostatin* expression relative to controls, indicating a possible mechanism whereby GHR signaling in muscle could affect liver and adipose tissue function. Thus, our study implicates skeletal muscle GHR signaling in mediating insulin resistance in obesity and, more importantly, reveals a novel role of muscle GHR signaling in facilitating cross-talk between muscle and other metabolic tissues. ***Diabetes*** **61:94–103, 2012**

The metabolic actions of growth hormone (GH) are largely attributed to the stimulation of lipolysis, and the subsequent rise in free fatty acid (FFA) flux from the adipose tissue resulting in increased FFA uptake and use in the skeletal muscle and liver (reviewed in 1,2). However, an inherent limitation to studies using global alteration of GH action is the accompanying change in body composition as well as changes in insulin-like growth factor (IGF)-1 and insulin action, complicating our ability to dissect the tissue-specific metabolic effects of GH.

From the [1]Division of Endocrinology, Diabetes, and Bone Diseases, the Department of Medicine, Mount Sinai School of Medicine, New York, New York; the [2]Departments of Medicine and Neuroscience, Albert Einstein College of Medicine, Bronx, New York; and the [3]Transgenic Core Facility, National Heart, Lung, and Blood Institute, National Institutes of Health, Bethesda, Maryland.

Corresponding authors: Derek LeRoith, derek.leroith@mssm.edu, and Shoshana Yakar, sy1007@nyu.edu.

Received 14 June 2011 and accepted 18 October 2011.

DOI: 10.2337/db11-0814

This article contains Supplementary Data online at http://diabetes.diabetesjournals.org/lookup/suppl/doi:10.2337/db11-0814/-/DC1.

A.V. and Y.W. contributed equally to this study.

Y.W., H.S., and S.Y. are currently affiliated with the David B. Kriser Dental Center, Department of Basic Science and Craniofacial Biology, New York University College of Dentistry, New York, New York.

An important aspect of the metabolic effects of GH is its ability to antagonize insulin action in the muscle, likely via the direct stimulation of negative regulators of insulin signaling such as suppressor of cytokine signaling (SOCS) proteins and p85α regulatory subunit of phosphatidylinositol 3-kinase (PI3K). SOCS proteins facilitate insulin resistance by several mechanisms including mediation of the proteasomal degradation of insulin receptor substrate (IRS) proteins that are involved in insulin/IGF-1 signal transduction (3). Excess GH levels have been associated with increased skeletal muscle expression of p85α, which can downregulate insulin signaling by preventing the activation of the p110 catalytic subunit of PI3K (4–6). On the other hand, GH-mediated increase in FFA flux into the muscle and its subsequent reesterification to triglycerides (TG) yield intermediates such as diacylglycerols and ceramides that can attenuate insulin signaling by activation of protein kinase C (PKC) isoforms (7).

To address the muscle-specific effects of the growth hormone receptor (GHR) on substrate metabolism and insulin action, we generated the mGHRKO mouse model with inactivation of *ghr* specifically in postnatal skeletal muscle using the Cre/loxP system. Our study implicates skeletal muscle GHR signaling in influencing substrate preference and maintenance of whole-body energy homeostasis, particularly in the obese state.

RESEARCH DESIGN AND METHODS

The generation of the GHR^{floxed} mice has been described elsewhere (8). The GHR^{floxed} mice were crossed with muscle creatine kinase (MCK-Cre) mice [cat. no. 006475 B6.FVB (129S4)-Tg(Ckmm-Cre)5Khn/J; The Jackson Laboratory, Bar Harbor, ME] to derive the mGHRKO mice (9). The mice were housed in the pathogen-free Association for the Assessment and Accreditation of Laboratory Animal Care International–accredited animal facilities of the Mount Sinai School of Medicine and were kept on a 12-h light/dark cycle. All experimental procedures were in accordance with the Institutional Animal Care and Use Committee of the Mount Sinai School of Medicine. Male mice on the C57BL/6 background were used for all experiments. The mice had ad libitum access to water and either a standard laboratory diet (LabDiet, Brentwood, MO) or a high-fat (60% fat) diet (HFD) (BioServ, New Brunswick, NJ). In all experiments, the mGHRKO ($GHR^{flox/flox}$; cre) mice were compared with control mice ($GHR^{flox/flox}$).

Semiquantitative PCR. Genomic DNA from various tissues of 7- to 8-week-old mice was extracted using the conventional phenol-chloroform method. DNA concentrations were determined using NanoDrop ND-1000 Spectrophotometer (Thermo Scientific, Wilmington, DE), and 500 ng DNA was subjected to semiquantitative PCR using the primer set 5′-CATTCTTTTCTGGGATGCTAT-3′ and 5′-CGGACATTGCATCTGTGATT-3′, which detects the floxed, wild-type, and null (recombinant) forms of the GHR.

In vivo stimulation. Mice were acutely stimulated with recombinant human growth hormone (rhGH) (Genentech, San Francisco, CA), insulin (Humulin R; Eli Lilly, Indianapolis, IN), IGF-1 (Genetech, San Francisco, CA), or 1× PBS, anesthetized with 2.5% Avertin (2,2,2-Tribromoethanol dissolved in *tert*-amyl alcohol; Sigma). The tissues were extracted, snap-frozen in liquid nitrogen, and subjected to Western blot analysis.

Growth parameters and circulating factors. Body composition analysis was performed using the EchoMRI 3-in-1 NMR system (Echo Medical Systems, Houston, TX). Body length was measured as nose-to-anus length at the time of sacrifice. Blood glucose level was measured from the tail using an automated glucometer (Elite; Bayer, Mishawaka, IN). Serum or plasma collected from the tail vein or retro-orbital sinus was used for measurement of circulating insulin (Linco, St. Charles, MO), IGF-1 (Alpco, Salem, NH), GH (Millipore, Bellirica, MA), FFA (Roche Applied Science, Indianapolis, IN), TG (Pointe Scientific, Canton, MI), interleukin (IL)-6, and adiponectin (R&D Systems, Minneapolis, MN) per the manufacturers' instructions.

Food intake, glucose and insulin tolerance tests, and hyperinsulinemic-euglycemic clamp. Food intake was measured weekly as previously published (10). Glucose and insulin tolerance tests were performed in unrestrained mice as previously described (10). Hyperinsulinemic-euglycemic clamps were performed in unrestrained mice fed HFD for 14–20 weeks as previously described (11).

Histology and immunoflourescence. Liver and epididymal fat pad were fixed in 10% PBS-buffered formalin; paraffin sections were processed and subjected to either hematoxylin-eosin (H-E) staining or immunoflorescence as previously described (12). For the immunoflourescence, F4/80 primary antibody (Abcam, Cambridge, MA) with Alexa Fluor goat anti-rat secondary antibody (Molecular Probes, Eugene, OR) was used. Pictures were obtained using the Olympus AX70 camera (Olympus, Center Valley, PA) at 10× objective magnification. ImageJ software (NIH, Bethesda, MD) was used to quantify the cross-sectional area of at least 150–250 adipocytes and fraction of the $F4/80^+$ area.

Western blot. Protein extraction from the liver, quadriceps, and epididymal fat pad and Western blot analyses were performed as previously described (10). The primary antibodies used were phosphorylated signal transducer and activator of transcription (Stat)5^{Tyr694}, phosphorylated IGF-1 receptor $\beta^{Tyr1135/1136}$/insulin receptor $\beta^{Tyr1150/1151}$, phosphorylated Akt^{Ser473}, Akt, phosphorylated p42/44 MAP $kinase^{Thr202/Tyr204}$ (phosphorylated extracellular signal–related kinase [Erk]), and p42/44 MAP kinase (Erk), phosphorylated AMP-activated protein kinase (AMPK)α^{Thr172}, and AMPKα from Cell Signaling Technology (Danvers, MA); STAT5, IRβ, IGF-IRβ, CD36, p85α, and β-tubulin from Santa Cruz Biotechnology (Santa Cruz, CA); and lipoprotein lipase (LPL) and SOCS-3 from Abcam (Cambridge, MA). Anti-rabbit secondary antibody from Li-cor Biosciences (Lincoln, NE) was used. The blots were quantified using the Odyssey Infrared Imaging System Application software (version 3.0; Li-cor Biosciences).

Gene expression analyses. Total RNA from quadriceps was extracted using TRIzol reagent and reverse transcribed according to the manufacturer's instructions (Invitrogen, Carlsbad, CA). Real time-PCR was performed using the QuantiTect SYBR green PCR kit (QIAGEN, Valencia, CA) in ABI PRISM 7900HT sequence detection systems (Applied Biosystems, Foster City, CA). The primers are listed in Supplementary Table 1; for each gene, a single sample was assayed three times and gene expression was normalized to *gapdh*.

Tissue TG and indirect calorimetry. Total TG were extracted from the liver and gastrocnemius using the chloroform-methanol method (13). TG content was quantified using TG reagent (Pointe Scientific, Canton, MI). Metabolic cage studies were performed in unrestrained mice fed an HFD for 12–14 weeks as previously described (11).

Statistical analysis. All results are expressed as means ± SEM. One-way (for comparison of two groups) or two-way ANOVA (for comparison of three or more groups) with Holm Sidak post hoc test was performed using SigmaStat for Windows (version 3.5; Systat Software, Inc., Chicago, IL).

RESULTS

mGHRKO mice harbor skeletal muscle–specific *ghr* gene inactivation. Skeletal muscle–specific *ghr* gene recombination in the mGHRKO mice was validated at the level of genomic DNA and mRNA expression (Fig. 1*A* and *B*). Acute rhGH (125 μg/kg i.p. for 15 min) stimulation elicited robust STAT5 phosphorylation in the muscle of control mice but not mGHRKO mice, while the livers of both control and mGHRKO mice displayed a similar response (Fig. 1*C*). Interestingly, loss of *ghr* in postnatal skeletal muscle did not affect muscle *igf-1* expression in the mGHRKO mice, and mice did not respond differently to an acute IGF-1 stimulation (1 mg/kg i.p. for 5 min) (Fig. 1*B* and Supplementary Fig. 1*E*). Moreover, circulating IGF-1 and GH levels and body length were similar between control and mGHRKO mice at 16 weeks of age (Table 1).

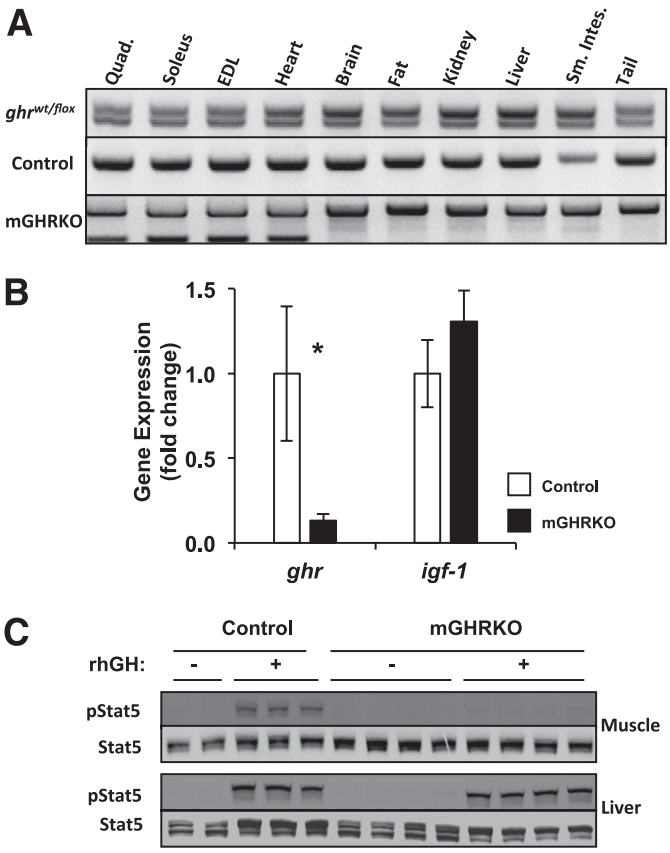

FIG. 1. mGHRKO mice have skeletal muscle–specific ablation of the *ghr* gene. *A*: Genomic DNA was isolated from the indicated tissues of 7- to 8-week-old control and mGHRKO mice, and recombination of *ghr* was assessed by semiquantitative PCR. The recombinant null *ghr* is expressed only in the various muscle groups and heart of the mGHRKO mice. *n* = 2–3/group. (Representative images are shown.) Quad, quadriceps; EDL, extensor digitorum longus; Sm. Intes, small intestine. *B*: Real-time PCR analysis of *ghr* and *igf-1* expression in quadriceps of 16-week-old control and mGHRKO mice. Gene expression was normalized to *gapdh* (*n* = 3–4/group). *C*: Acute GH stimulation (125 μg/kg body wt i.p. for 15 min) of 7- to 8-week-old mice and probing for STAT5 phosphorylation in the liver and quadriceps by immunoblot analysis. Phosphorylated levels of STAT5 (pSTAT5) were normalized to total STAT5 levels (*n* = 2–4/group). **P* ≤ 0.05, one-way ANOVA.

mGHRKO mice are protected against HFD-induced insulin resistance. The lean mGHRKO mice displayed reduced body weight in adulthood, starting at 7 weeks of age (Supplementary Fig. 1*A*). HFD feeding starting at 5–7 weeks of age increased body weights of both the control and mGHRKO mice relative to the lean mice; however, the obese mGHRKO mice were significantly lighter than the obese control mice (Fig. 2*A*). Absolute lean mass was significantly decreased in both lean and obese mGHRKO mice compared with the control mice (Fig. 2*B*). However, while the lean mGHRKO mice had lower absolute fat mass than the lean control mice (Supplementary Fig. 1*B*), relative body adiposity was significantly reduced only in the obese mGHRKO mice compared with the obese control mice (Fig. 2*C*). The lower body weight and fat mass in the obese mGHRKO mice could not be explained by lower food intake, which was similar in both groups (Supplementary Fig. 2*A*). Moreover, wet tissue weights of the gonadal and subcutaneous fat pads were also significantly decreased in the lean and obese mGHRKO mice compared with their respective controls (Table 1). The obese mGHRKO mice demonstrated lower circulating

TABLE 1
Characterization of lean and obese control and mGHRKO mice

	Lean		Obese	
	Control	mGHRKO	Control	mGHRKO
Body length, n = 4–10 (cm)	9.91 ± 0.04	10.08 ± 0.08	10.25 ± 0.16	10.02 ± 0.16
GH, n = 6–7 (ng/mL)	11.84 ± 8.38	9.24 ± 5.11	n.d.	n.d.
IGF-1, n = 7–10 (ng/mL)	316.29 ± 6.27	309.50 ± 8.90	n.d.	n.d.
Fed state blood glucose, n = 18–33 (mg/dL)	150.04 ± 4.50	129.73 ± 3.36*	163.05 ± 6.22	158.78 ± 5.76
Fed state FFA, n = 9–15 (nmol/μL)	0.40 ± 0.03	0.30 ± 0.08*	0.32 ± 0.02	0.39 ± 0.04
Gonadal fat pad weight, n = 14–27 (g)	0.596 ± 0.04	0.446 ± 0.03*	2.93 ± 0.14	2.34 ± 0.08*
Subcutaneous fat pad weight, n = 7–27 (g)	0.319 ± 0.02	0.229 ± 0.02*	1.95 ± 0.22	1.21 ± 0.07*
IL-6, n = 4–29 (pg/mL)	6.25 ± 2.33	13.57 ± 4.07	19.80 ± 4.13	9.91 ± 1.56*
Adiponectin, n = 4–41 (ng/mL)	2.87 ± 0.32	3.83 ± 0.08*	4.59 ± 0.21	4.73 ± 0.17

Data are means ± SEM. n.d., not determined. *$P \leq 0.05$ control vs. mGHRKO, one-way ANOVA.

TG levels compared with the obese controls, and while the lean mGHRKO mice had reduced circulating FFA levels compared with controls, no difference was observed in the obese mice (Table 1). Like the lean mice, the obese control, but not obese mGHRKO, mice displayed robust muscle STAT5 phosphorylation in response to acute rhGH stimulation (125 μg/kg i.v. for 10 min), while the hepatic response was similar between the two groups (Supplementary Fig. 2*B*).

We next sought to determine whether the reduced body weight and fat mass in the lean and obese mGHRKO mice translated into better metabolic outcomes. Despite significantly lower fed-state blood glucose levels (Table 1), the lean mGHRKO mice did differ from the lean controls in their serum insulin levels or response to a glucose tolerance test, an insulin tolerance test, or acute insulin stimulation (Fig. 2*D* and Supplementary Fig. 1*C*–*E*). However, the obese mGHRKO mice had significantly lower insulin levels than did the obese control mice (Fig. 2*D*) and demonstrated improved insulin sensitivity during glucose tolerance and insulin tolerance tests (Fig. 2*E* and *F*).

Consequently, the obese mGHRKO and control mice were subjected to hyperinsulinemic-euglycemic clamps to determine which tissue(s) contributed to the improved insulin sensitivity. The obese mGHRKO mice demonstrated improved hepatic insulin sensitivity, as evidenced by higher glucose infusion rate (GIR) and greater extent of insulin-mediated suppression of hepatic glucose production (HGP) (Fig. 3*A* and *B*). The obese mGHRKO mice also had an increased rate of whole-body glucose disposal (R_d), with a twofold increase in insulin-stimulated muscle and white adipose tissue glucose uptake compared with the control mice during the clamp period (Fig. 3*C*–*E*). Furthermore, Akt phosphorylation in response to acute insulin stimulation (1 unit/kg i.p. for 5 min) was significantly greater or tended to be higher in the adipose tissue and skeletal muscle, respectively, of the obese mGHRKO mice relative to the obese controls (Fig. 3*F* and *G*). Nonetheless, p85α protein content, which inversely correlates with insulin sensitivity, did not differ between the muscles of the obese control and mGHRKO mice (Supplementary Fig. 2*C*).

The reduced fat mass in the obese mGHRKO mice was associated with smaller adipocytes compared with the obese controls (Fig. 4*A*). Furthermore, the obese mGHRKO mice displayed significantly lower circulating IL-6 levels as well as adipose tissue macrophage infiltration, as assessed by F/480 staining, suggesting reduced obesity-associated inflammation (Table 1 and Fig. 4*B*). Interestingly, the lean mGHRKO mice displayed significantly higher serum adiponectin levels compared with the lean control mice; however, there was no difference in adiponectin levels in the obese mice (Table 1). Lean mGHRKO mice had similar liver and muscle TG content compared to lean controls. However, while HFD feeding increased tissue TG content in both groups, the obese mGHRKO mice had significantly less liver and muscle TG content than did the obese controls (Fig. 4*C* and *E*). In concordance with this, the obese control but not obese mGHRKO mice developed marked hepatic steatosis (Fig. 4*D*).

Obese mGHRKO mice demonstrate improved metabolic efficiency. The reduced body adiposity in the obese mGHRKO mice was associated with improved insulin sensitivity, which may result from increased metabolic efficiency (analyzed by indirect calorimetry). As hypothesized, the obese mGHRKO mice showed increased light- and dark-phase oxygen consumption (VO_2) (Fig. 5*A*) and CO_2 production (VCO_2) (Fig. 5*B*), resulting in a higher respiratory exchange ratio (Fig. 5*C*) suggestive of greater carbohydrate utilization. The obese mGHRKO mice also demonstrated greater energy expenditure in both the light and the dark phases (Fig. 5*D*). The mGHRKO mice had increased locomotor activity, which may have further contributed to their increased energy expenditure (data not shown).

Skeletal muscle lipid metabolism is improved in obese mGHRKO mice relative to obese controls. GH has known roles in lipid uptake and metabolism, and the obese mGHRKO mice also displayed lower muscle TG content. We subsequently found a reduction in the expression of genes involved in de novo lipogenesis and TG reesterification such as fatty acid synthase *(fasn)*, sterol regulatory binding protein-1 *(srebp-1)*, and diglyceride acyltransferase-1 *(dgat1)* in the obese mGHRKO muscles relative to controls (Fig. 6*A*). There was no difference in the expression of β-oxidation markers such as carnitine palmitoyltransferase 1-α (*cpt1α*) and peroxisome proliferator–activated receptor γ coactivator 1-α (*pgc1α*) (Fig. 6*A*). Additionally, protein content of LPL and the fatty acid transporter CD36, which are involved in fatty acid uptake, did not differ between the obese control and mGHRKO mice (Supplementary Fig. 2*C*).

Altered expression of muscle markers in mGHRKO mice that could contribute to their insulin sensitivity. SOCS proteins are negative regulators of insulin signaling, and we found a reduction in the mRNA expression of *socs2* but not *socs1* in the obese mGHRKO mice (Fig. 6*B*). There

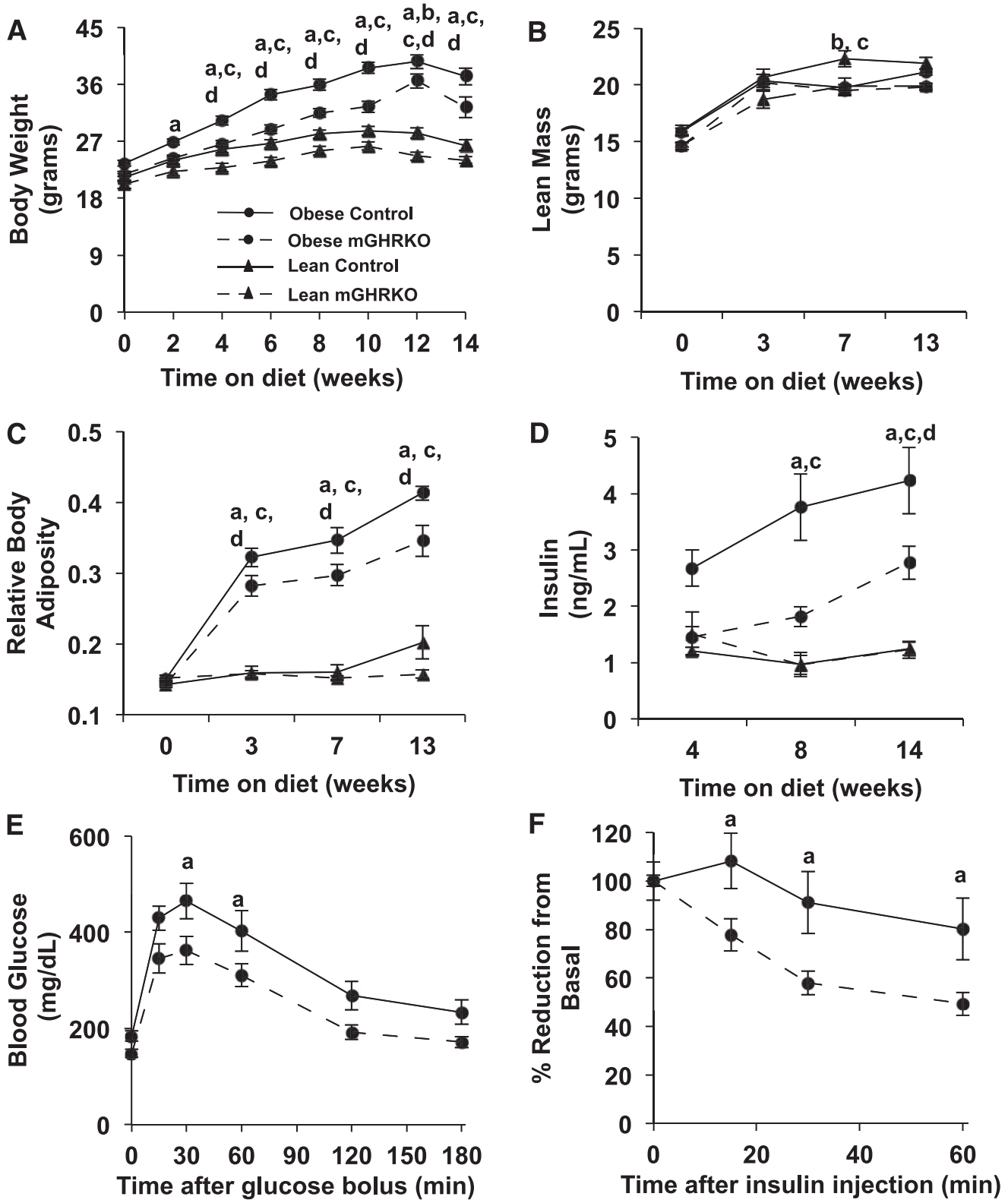

FIG. 2. Obese mGHRKO mice have reduced adiposity and improved insulin sensitivity. Control and mGHRKO mice were placed on an HFD (60% of calories from fat) starting at 5–7 weeks of age and were compared with littermates fed a standard laboratory diet. *A*: Body weight. *B*: Lean body mass. *C*: Relative body adiposity. *D*: Circulating insulin levels of lean and obese control and mGHRKO mice were measured at indicated times (n = 9–18/group). Glucose tolerance (1 g/kg) (*E*) and insulin tolerance (0.5 units/kg) (*F*) tests in mice fed an HFD for 22 weeks (n = 10/group). All values are represented as means ± SEM. [a]$P \leq 0.05$ for obese control vs. obese mGHRKO, [b]$P \leq 0.05$ for lean control vs. lean mGHRKO, [c]$P \leq 0.05$ for lean control vs. obese control, [d]$P \leq 0.05$ for lean mGHRKO vs. obese mGHRKO; one- and two-way ANOVA.

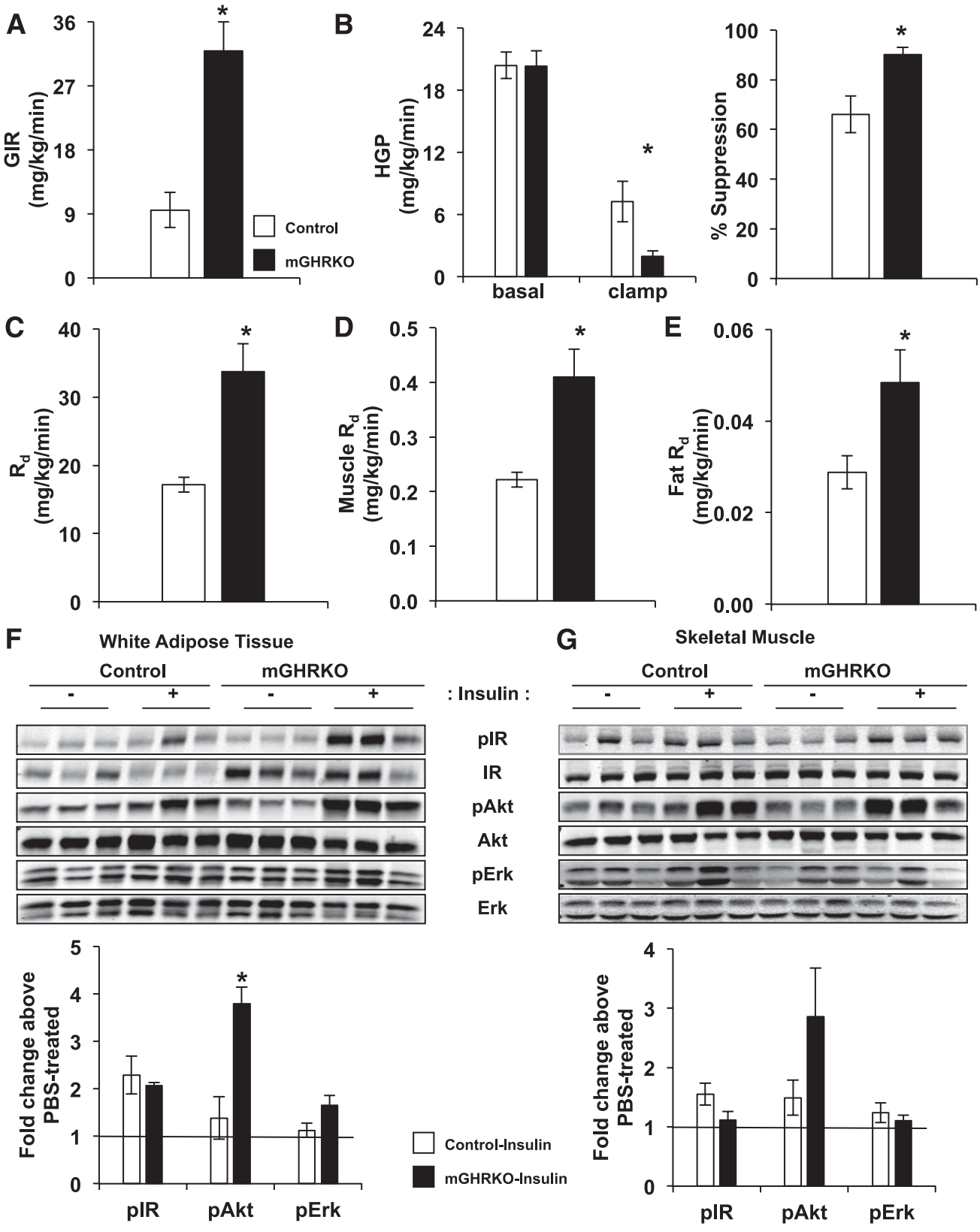

FIG. 3. Improved insulin sensitivity in obese mGHRKO mice as assessed by hyperinsulinemic-euglycemic clamps. Mice were placed on an HFD (60% of calories from fat) starting at 5–7 weeks of age and were subjected to hyperinsulinemic-euglycemic clamps after 12–14 weeks of HFD feeding. *A*: GIR. *B*: HGP at basal and insulin-stimulated states (*left panel*) and extent of insulin-mediated suppression of HGP (*right panel*). *C*: Whole-body R_d. *D*: Skeletal muscle R_d. *E*: Adipose tissue R_d (fat R_d) at the end of the clamp period was measured (n = 5/group for all clamp studies). *F* and *G*: Immunoblot analysis of white adipose tissue (*F*) and skeletal muscle (G) response to an acute insulin (1 unit/kg i.p. for 5 min) stimulation of mice fed an HFD as evaluated by phosphorylation of insulin receptor (pIR), Akt (pAkt), and Erk (pErk), which are normalized to total protein levels (n = 3–4 /group). The blots were quantified and represented as the extent of stimulation with respect to PBS-treated levels for each group. All values are represented as means ± SEM. *$P \leq 0.05$, one-way ANOVA.

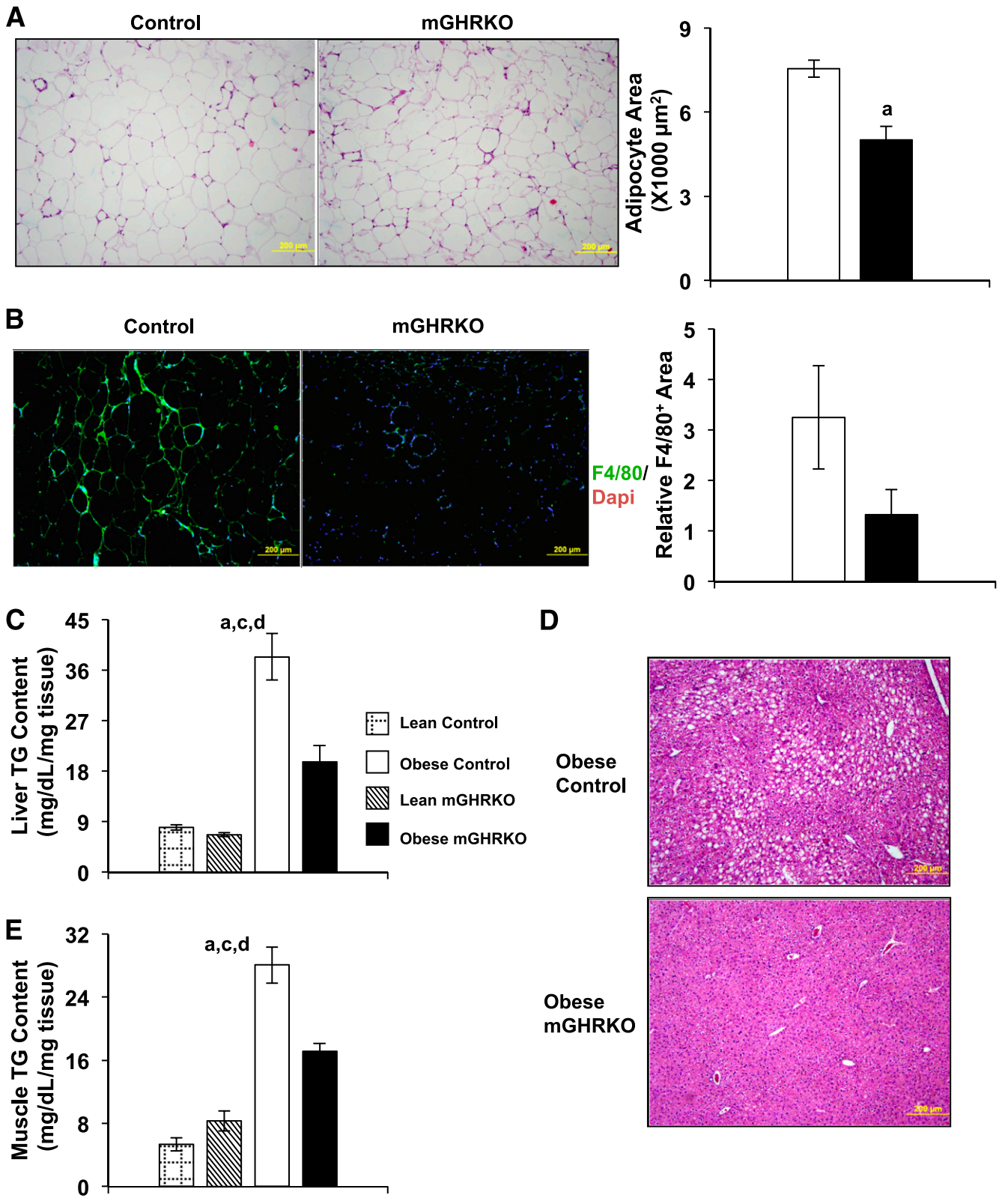

FIG. 4. mGHRKO mice are protected from complications of HFD-induced insulin resistance and obesity. Mice were placed on an HFD (60% of calories from fat) starting at 5–7 weeks of age for a period of 14 weeks and, where indicated, were compared with lean mice. *A*: Adipocyte area as evaluated by H-E staining (*right panel*) and the area of 150–200 adipocytes were quantified using the NIH ImageJ software (*left panel*) (n = 7/group). (Representative images are shown.) *B*: Immunoflourescent staining for F4/80$^+$ adipocytes in epididymal adipose tissue; the fraction of F4/80$^+$ area was quantified using the NIH ImageJ software (n = 7/group). (Representative images are shown.) *C*: Liver TG content (n = 6–11/group). *D*: Hepatic steatosis as evaluated by H-E staining (n = 6–7/group). (Representative images are shown.) *E*: Muscle TG content determined in the gastrocnemius (n = 6–11/group). In all of the images, the scale bar represents 200 µm. All values are represented as means ± SEM. $^aP \le 0.05$ for obese control vs. obese mGHRKO, $^bP \le 0.05$ for lean control vs. lean mGHRKO, $^cP \le 0.05$ for lean control vs. obese control, $^dP \le 0.05$ for lean mGHRKO vs. obese mGHRKO; one- and two-way ANOVA. (A high-quality color representation of this figure is available in the online issue.)

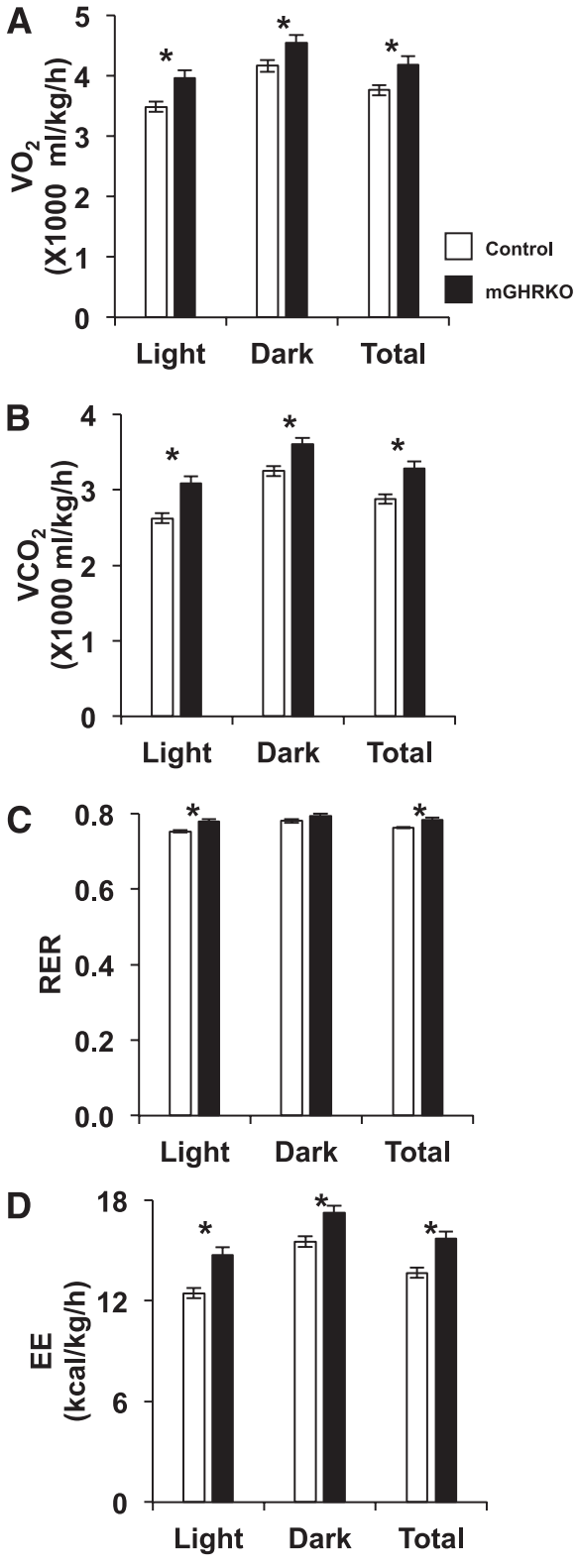

FIG. 5. Obese mGHRKO mice are more metabolically efficient than obese controls. Mice were placed on an HFD (60% of calories from fat) starting at 5–7 weeks of age for a period of 14 weeks, and their thermodynamic properties were studied in metabolic cages. *A*: Oxygen consumption (VO_2). *B*: CO_2 production (VCO_2). *C*: Respiratory exchange ratio (RER). *D*: Energy expenditure (EE) (n = 8/group). All values are represented as means ± SEM. *$P \leq 0.05$, one-way ANOVA.

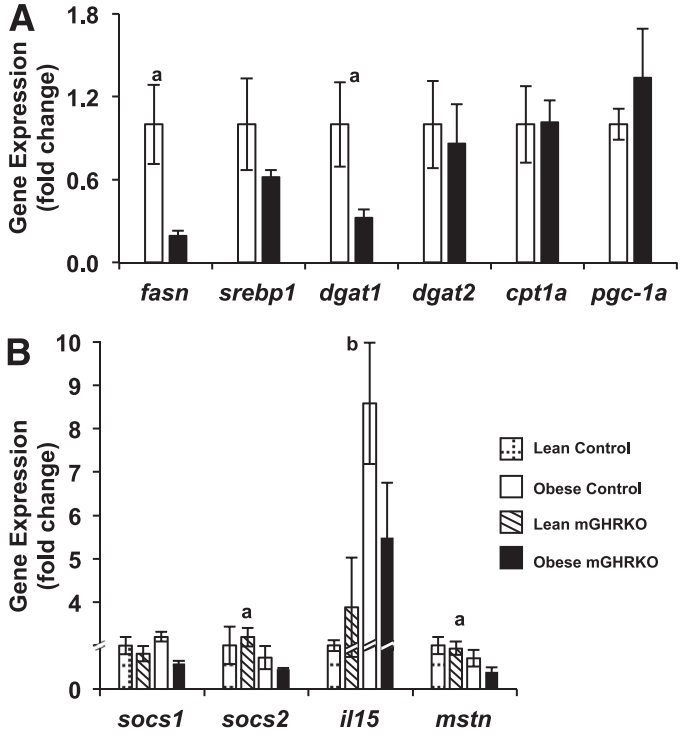

FIG. 6. Altered gene expression in the obese mGHRKO muscles. Mice were placed on an HFD (60% of calories from fat) starting at 5–7 weeks of age for a period of 14 weeks, and the quadriceps muscles were analyzed. *A*: Real-time PCR analysis of indicated genes is represented as fold change compared with expression of obese control mice. Gene expression was normalized to *gapdh* (n = 4–5/group). *B*: Expression of *socs2*, *socs1*, *mstn*, and *il-15* in muscles of lean and obese control and mGHRKO mice was quantified by real-time PCR, normalized to *gapdh*, and represented as fold change compared with expression in lean control mice (n = 3–5/group). The double line on the y-axis denotes where the scale was broken. All values are represented as means ± SEM. [a]$P \leq 0.05$ for obese control vs. obese mGHRKO, [b]$P \leq 0.05$ for lean control vs. lean mGHRKO; one- and two-way ANOVA.

was also no difference in protein content of SOCS3 in the obese control and mGHRKO mice (Supplementary Fig. 2*C*).

Additionally, the expression of myostatin *(mstn)* and *il-15* was reduced and increased, respectively, in the skeletal muscles of the mGHRKO mice (Fig. 6*B*). There was no difference in AMPK phosphorylation between the lean and obese mice of both groups (data not shown).

DISCUSSION

Herein, we report that loss of skeletal muscle GHR signaling improves insulin sensitivity in the context of diet-induced obesity. While HFD feeding worsened the metabolic state of both control and mGHRKO mice compared with their lean counterparts, the obese mGHRKO mice demonstrated significantly lower body weight, body adiposity, and insulin resistance relative to the obese controls. Hyperinsulinemic-euglycemic clamp studies indicated increased GIR and muscle and adipose tissue R_d in obese mGHRKO mice compared with obese controls. These data were substantiated with greater insulin-stimulated Akt phosphorylation in the white adipose tissue and muscle of the obese mGHRKO mice. Further, indirect calorimetry studies revealed greater energy expenditure, which was associated with greater carbohydrate utilization in the obese mGHRKO mice.

The improved insulin sensitivity of the obese mGHRKO mice could have arisen as a consequence of direct GH

action in the skeletal muscle or indirectly as a result of improvements in other tissues such as the liver and adipose tissue. As we discuss below, our data with the mGHRKO mice provide a rationale for both possibilities.

The obese mGHRKO mice demonstrate increased insulin-stimulated skeletal muscle glucose uptake and a shift in substrate utilization toward increased carbohydrate metabolism. Moreover, the obese mGHRKO mice had lower muscle TG content, which could reflect either reduced lipid uptake into the skeletal muscle or increased lipid oxidation. GH has been shown to reduce LPL activity in the adipose tissue and, thus, suppress adipose tissue lipid uptake, but its effect on muscle LPL activity is not well characterized (14–17). Accordingly, we did not find a difference in LPL protein content in the obese mGHRKO mice compared with the obese controls. The protein content of the fatty acid transporter CD36, which is also regulated by subcellular localization (18,19), was also not different between the obese control and mGHRKO mice. Furthermore, we found reduced expression of genes involved in de novo lipogenesis and TG reesterification in the obese mGHRKO muscles, while expression of genes involved in β-oxidation was not different. Nevertheless, protein content or mRNA expression does not reflect substrate flux, which could be different between the obese mGHRKO and control muscles. Muscle TG content is inversely correlated with insulin sensitivity because of accumulation of intermediates such as diacylglycerols and ceramides that can inhibit insulin signaling by activation of PKC isoforms (7). Thus, lower muscle TG content in the obese mGHRKO mice could potentially account for enhanced muscle insulin sensitivity in the face of HFD feeding.

GH can interfere with insulin signaling by inducing the expression of SOCS proteins, especially SOCS2 and SOCS3 (3,20,21). Accordingly, muscles of obese mGHRKO mice had decreased *socs2* but not *socs1* mRNA expression. Thus, lower *socs2* expression could, to some degree, explain the increased insulin action in the mGHRKO muscles. The p85α regulatory subunit of PI3K is regulated by GH and is overexpressed in the insulin-resistant muscle, where it is hypothesized to bind to and sequester IRS-1, thereby preventing the activation of the p110 catalytic subunit of PI3K. While total protein content of p85α did not differ between the obese control and mGHRKO mice, we could not determine whether the p85α levels that we detected represent its monomeric or homo/hetero-dimeric forms in the obese control versus mGHRKO muscles.

A recent study by Mavalli et al. (22) reported that knockout of the GHR in skeletal muscle using the myocyte-specific enhancer factor 2C promoter resulted in enhanced body weight, body adiposity, and circulating TG levels and worsened insulin sensitivity. While the knockout mice demonstrated decreased dark-phase locomotor activity, they tended to have increased energy expenditure. Moreover, primary myotubes isolated from the knockout mice demonstrated decreased insulin-stimulated glucose uptake, insulin receptor protein content, and basal Akt (Thr 308 but not Ser 473) and Erk phosphorylation. Interestingly, primary myoblast cultures isolated from the knockout mice displayed reduced inhibitory Ser phosphorylation of IRS-1 at residues 612 and 636/639, while Ser phosphorylation of residue 1101, which is regulated by the diacylglycerol-responsive PKCθ, was higher (23). These data are contrary to our observations in the mGHRKO mice, which had reduced fat mass and slightly improved metabolism under lean conditions and were protected from HFD-induced insulin resistance. Moreover, we did not observe any difference in insulin receptor content or basal Akt or Erk phosphorylation in whole-muscle tissue lysates of the lean mGHRKO mice.

The discrepancies between the two studies may arise from the different genetic background of the mice used; the strain-specific differences in metabolic response are well documented (24). Additionally, the MCK promoter used to drive the Cre recombinase expression in the mGHRKO mice is expressed primarily in postnatal skeletal and cardiac muscle (25). The myocyte-specific enhancer factor 2C promoter, while expressed only in the skeletal muscle postnatally (26), is also expressed prenatally at 7.5 days postconception in the heart and regions that develop into the brain (27). Thus, it is conceivable that changes arising from early inactivation of the GHR in the developing somite may influence the phenotype of the mice in adulthood. Further, the molecular data presented by Mavalli et al. were generated in an in vitro system using primary myoblasts isolated at 4 weeks of age, when the knockout mice do not demonstrate an insulin-resistant phenotype in vivo. On the other hand, our experiments were performed in whole tissue lysates isolated at either 16 weeks of age or 14 weeks of HFD feeding, when the mGHRKO mice showed a clear phenotype.

Inactivation of *stat5a/b* in the skeletal muscle using the Myf5 promoter to drive Cre expression resulted in reduced body length and body weight (primarily due to a reduction in lean mass) and worsened glucose tolerance (28). However, similar to the above-mentioned study, these mice were on a mixed genetic background and the Myf5 promoter was also expressed prenatally at 8 days postconception (29). Moreover, while GH is one of the major activators of STAT5, other factors, including insulin, can also induce this transcription factor (30,31); furthermore, GH does not signal exclusively through STAT5 (32).

An interesting point of comparison between our observations and the two aforementioned studies is muscle *igf-1* expression in the knockout mice. While we did not observe a difference in *igf-1* expression in adult mGHRKO mice, both of the other studies reported a significant reduction in muscle *igf-1* expression. Moreover, the muscle-*stat5 a/b* knockout mice also demonstrated a 15% reduction in circulating IGF-1 levels. This suggests that muscle *igf-1* expression is regulated by GH prenatally but not postnatally. Indeed, studies performed in both in vitro and in vivo settings have reported GH-independent changes in expression of the different IGF-1 isoforms under various experimental conditions (33–36).

Another significant difference between the findings of the study by Mavalli et al. and those in the mGHRKO mice is that while the former reported increased body adiposity, we observed the opposite in the mGHRKO mice. Thus, it is very possible that the difference in adiposity may be responsible for the difference in insulin sensitivity between the two models. Moreover, the obese mGHRKO mice also demonstrated increased adipose tissue and hepatic insulin sensitivity in the hyperinsulinemic-euglycemic clamp studies, as well as reduced adipose tissue macrophage infiltration, liver TG content, and circulating TG levels. The obese mGHRKO mice had significant reductions in circulating IL-6 levels, an adipocytokine associated with obesity-induced systemic inflammation insulin resistance (37). Circulating adiponectin levels, which positively correlate with insulin sensitivity (37) and may influence muscle metabolism by promoting the

deacetylation of PGC-1α (38), were increased in the lean but not obese mGHRKO mice. All these factors could have a major impact on the insulin sensitivity of the obese mGHRKO mice.

An interesting implication of our study is that GH facilitates tissue cross-talk, possibly via the regulation of secreted myokines that affect adipose tissue and liver metabolism. Indeed, we found a reduction in the expression of *mstn* in the mGHRKO mice. Whole-body and skeletal muscle–specific myostatin knockout mice demonstrated improved insulin sensitivity and protection from HFD-induced obesity and insulin resistance (39–41). The improved insulin sensitivity in the myostatin knockout mice was attributed to increased AMPK phosphorylation and energy expenditure (40,42). However, while the obese mGHRKO mice displayed increased energy expenditure we could not detect an increase in AMPK phosphorylation in the lean or obese mGHRKO mice. Further, Oldham et al. (43) reported that GH may regulate myostatin mRNA and protein expression via STAT5-dependent and -independent mechanisms. We also observed an increase in *il-15* expression in the lean and obese mGHRKO mice. Unlike myostatin, IL-15 positively affects metabolism by modulating substrate metabolism in the liver, white adipose tissue, and brown adipose tissue (44). While we had technical difficulties in validating our mRNA expression levels at the protein level, these preliminary findings nevertheless provide exciting new areas for future research.

Obesity is often described as a GH-suppressed state. Given this, it is paradoxical that we observed strong metabolic improvements in the obese mGHRKO mice. Mean peak GH levels, GH pulse amplitude, and the rate of GH secretion (but not the frequency of GH pulses) have been shown to be reduced in obese individuals (45,46). Further, obese, insulin-resistant mice are responsive to an acute GH stimulation. Likewise, obese women treated with GH respond in a similar manner to nonobese women in terms of fat loss and the suppression of adipose tissue LPL activity (18). Thus, obesity is associated with reduced but not absent GH secretion, and the metabolic action of GH may still persist in this state.

In conclusion, through use of mGHRKO mice we describe roles for muscle GHR signaling in mediating whole-body insulin resistance in obesity. This may occur via alterations in substrate utilization and energy expenditure. An interesting implication of our study is the effect that loss of GHR signaling in the muscle has on other metabolic tissues, such as the adipose tissue and liver, which bears further investigation.

ACKNOWLEDGMENTS

X.L. and G.J.S. are supported by the NIH DK-20541 grant from the National Institutes of Health.

No potential conflicts of interest relevant to this article were reported.

A.V. designed and performed the experiments and wrote the manuscript. Y.W. designed and performed the experiments and reviewed and edited the manuscript. H.S., X.L., Z.J., and C.L. performed the experiments. G.J.S. and S.Y. designed the experiments, reviewed and edited the manuscript, and contributed to discussion. D.L. designed the experiments, reviewed and edited the manuscript, contributed to discussion, and is the guarantor.

The authors thank Caroline Kornhauser, Yosef Chodakiewitz, Darren Gorman, Joshua Vazhapilly, Dr. Emily Gallagher, and Dr. Rosalyn Ferguson from the Mount Sinai School of Medicine for their assistance with the experiments and review of the manuscript.

Parts of this study were presented in abstract form at the 93rd Annual Meeting of The Endocrine Society, Boston, MA, 4–7 June 2011, and the 5th International Congress of the GRS and IGF Society, New York, NY, 3–7 October 2010.

REFERENCES

1. Møller N, Jørgensen JO. Effects of growth hormone on glucose, lipid, and protein metabolism in human subjects. Endocr Rev 2009;30:152–177
2. Vijayakumar A, Yakar S, LeRoith D. The intricate role of growth hormone in metabolism. Front Endocrin 2011;2:32
3. Howard JK, Flier JS. Attenuation of leptin and insulin signaling by SOCS proteins. Trends Endocrinol Metab 2006;17:365–371
4. Mauvais-Jarvis F, Ueki K, Fruman DA, et al. Reduced expression of the murine p85alpha subunit of phosphoinositide 3-kinase improves insulin signaling and ameliorates diabetes. J Clin Invest 2002;109:141–149
5. Ueki K, Fruman DA, Brachmann SM, Tseng YH, Cantley LC, Kahn CR. Molecular balance between the regulatory and catalytic subunits of phosphoinositide 3-kinase regulates cell signaling and survival. Mol Cell Biol 2002;22:965–977
6. Barbour LA, Mizanoor Rahman S, Gurevich I, et al. Increased P85alpha is a potent negative regulator of skeletal muscle insulin signaling and induces in vivo insulin resistance associated with growth hormone excess. J Biol Chem 2005;280:37489–37494
7. Samuel VT, Petersen KF, Shulman GI. Lipid-induced insulin resistance: unravelling the mechanism. Lancet 2010;375:2267–2277
8. Wu Y, Liu C, Sun H, Vijayakumar A, Giglou PR, Qiao R, Oppenheimer J, Yakar S, Leroith D. Growth hormone receptor regulates β cell hyperplasia and glucose-stimulated insulin secretion in obese mice. J Clin Invest 2011; 121:2422–2426
9. Brüning JC, Michael MD, Winnay JN, et al. A muscle-specific insulin receptor knockout exhibits features of the metabolic syndrome of NIDDM without altering glucose tolerance. Mol Cell 1998;2:559–569
10. Fierz Y, Novosyadlyy R, Vijayakumar A, Yakar S, LeRoith D. Insulin-sensitizing therapy attenuates type 2 diabetes-mediated mammary tumor progression. Diabetes 2010;59:686–693
11. Li X, Wu X, Camacho R, Schwartz GJ, LeRoith D. Intracerebroventricular leptin infusion improves glucose homeostasis in lean type 2 diabetic MKR mice via hepatic vagal and non-vagal mechanisms. PLoS ONE 2011;6:e17058
12. Cannata D, Lann D, Wu Y, et al. Elevated circulating IGF-I promotes mammary gland development and proliferation. Endocrinology 2010;151: 5751–5761
13. Kim H, Pennisi PA, Gavrilova O, et al. Effect of adipocyte beta3-adrenergic receptor activation on the type 2 diabetic MKR mice. Am J Physiol Endocrinol Metab 2006;290:E1227–E1236
14. Khalfallah Y, Sassolas G, Borson-Chazot F, Vega N, Vidal H. Expression of insulin target genes in skeletal muscle and adipose tissue in adult patients with growth hormone deficiency: effect of one year recombinant human growth hormone therapy. J Endocrinol 2001;171:285–292
15. Richelsen B. Effect of growth hormone on adipose tissue and skeletal muscle lipoprotein lipase activity in humans. J Endocrinol Invest 1999;22 (Suppl):10–15
16. Johansen T, Richelsen B, Hansen HS, Din N, Malmlöf K. Growth hormone-mediated breakdown of body fat: effects ofgrowth hormoneon lipases in adipose tissue and skeletal muscle of old rats fed different diets. Horm Metab Res 2003;35:243–250
17. Richelsen B, Pedersen SB, Børglum JD, Møller-Pedersen T, Jørgensen J, Jørgensen JO. Growth hormone treatment of obese women for 5 wk: effect on body composition and adipose tissue LPL activity. Am J Physiol 1994; 266:E211–E216
18. Schenk S, Horowitz JF. Coimmunoprecipitation of FAT/CD36 and CPT I in skeletal muscle increases proportionally with fat oxidation after endurance exercise training. Am J Physiol Endocrinol Metab 2006;291:E254–E260
19. Wang Y, Van Oort MM, Yao M, Van der Horst DJ, Rodenburg KW. Insulin and chromium picolinate induce translocation of CD36 to the plasma membrane through different signaling pathways in 3T3-L1 adipocytes, and with a differential functionality of the CD36. Biol Trace Elem Res 2011;142: 735–747
20. Greenhalgh CJ, Rico-Bautista E, Lorentzon M, et al. SOCS2 negatively regulates growth hormone action in vitro and in vivo. J Clin Invest 2005; 115:397–406
21. Nielsen C, Gormsen LC, Jessen N, et al. Growth hormone signaling in vivo in human muscle and adipose tissue: impact of insulin, substrate background,

and growth hormone receptor blockade. J Clin Endocrinol Metab 2008; 93:2842–2850
22. Mavalli MD, DiGirolamo DJ, Fan Y, et al. Distinct growth hormone receptor signaling modes regulate skeletal muscle development and insulin sensitivity in mice. J Clin Invest 2010;120:4007–4020
23. Gual P, Le Marchand-Brustel Y, Tanti JF. Positive and negative regulation of insulin signaling through IRS-1 phosphorylation. Biochimie 2005;87:99–109
24. Ayala JE, Samuel VT, Morton GJ, et al.; NIH Mouse Metabolic Phenotyping Center Consortium. Standard operating procedures for describing and performing metabolic tests of glucose homeostasis in mice. Dis Model Mech 2010;3:525–534
25. Caplan AI, Fiszman MY, Eppenberger HM. Molecular and cell isoforms during development. Science 1983;221:921–927
26. Vong LH, Ragusa MJ, Schwarz JJ. Generation of conditional Mef2cloxP/loxP mice for temporal- and tissue-specific analyses. Genesis 2005;43:43–48
27. Naya FJ, Wu C, Richardson JA, Overbeek P, Olson EN. Transcriptional activity of MEF2 during mouse embryogenesis monitored with a MEF2-dependent transgene. Development 1999;126:2045–2052
28. Klover P, Hennighausen L. Postnatal body growth is dependent on the transcription factors signal transducers and activators of transcription 5a/b in muscle: a role for autocrine/paracrine insulin-like growth factor I. Endocrinology 2007;148:1489–1497
29. Ott MO, Bober E, Lyons G, Arnold H, Buckingham M. Early expression of the myogenic regulatory gene, myf-5, in precursor cells of skeletal muscle in the mouse embryo. Development 1991;111:1097–1107
30. Ross JA, Cheng H, Nagy ZS, Frost JA, Kirken RA. Protein phosphatase 2A regulates interleukin-2 receptor complex formation and JAK3/STAT5 activation. J Biol Chem 2010;285:3582–3591
31. Sawka-Verhelle D, Tartare-Deckert S, Decaux JF, Girard J, Van Obberghen E. Stat 5B, activated by insulin in a Jak-independent fashion, plays a role in glucokinase gene transcription. Endocrinology 2000;141:1977–1988
32. Barclay JL, Kerr LM, Arthur L, et al. In vivo targeting of the growth hormone receptor (GHR) Box1 sequence demonstrates that the GHR does not signal exclusively through JAK2. Mol Endocrinol 2010;24:204–217
33. Ahtiainen JP, Lehti M, Hulmi JJ, et al. Recovery after heavy resistance exercise and skeletal muscle androgen receptor and insulin-like growth factor-I isoform expression in strength trained men. J Strength Cond Res 2011;25:767–777
34. Chen CN, Khor GT, Chen CH, Huang P. Wallenberg's syndrome with proximal quadriparesis. Neurologist 2011;17:44–46
35. Gentile MA, Nantermet PV, Vogel RL, et al. Androgen-mediated improvement of body composition and muscle function involves a novel early transcriptional program including IGF1, mechano growth factor, and induction of beta-catenin. J Mol Endocrinol 2010;44:55–73
36. Ostrovsky O, Eletto D, Makarewich C, Barton ER, Argon Y. Glucose regulated protein 94 is required for muscle differentiation through its control of the autocrine production of insulin-like growth factors. Biochim Biophys Acta 2010;1803:333–341
37. Galic S, Oakhill JS, Steinberg GR. Adipose tissue as an endocrine organ. Mol Cell Endocrinol 2010;316:129–139
38. Iwabu M, Yamauchi T, Okada-Iwabu M, et al. Adiponectin and AdipoR1 regulate PGC-1alpha and mitochondria by Ca(2+) and AMPK/SIRT1. Nature 2010;464:1313–1319
39. Guo T, Jou W, Chanturiya T, Portas J, Gavrilova O, McPherron AC. Myostatin inhibition in muscle, but not adipose tissue, decreases fat mass and improves insulin sensitivity. PLoS ONE 2009;4:e4937
40. Zhang C, McFarlane C, Lokireddy S, Bonala S, Ge X, Masuda S, Gluckman PD, Sharma M, Kambadur R. Myostatin-deficient mice exhibit reduced insulin resistance through activating the AMP-activated protein kinase signalling pathway. Diabetologia 2011;54:1491–1501
41. McPherron AC. Metabolic functions of myostatin and Gdf11. Immunol Endocr Metab Agents Med Chem 2010;10:217–231
42. Choi SJ, Yablonka-Reuveni Z, Kaiyala KJ, Ogimoto K, Schwartz MW, Wisse BE. Increased energy expenditure and leptin sensitivity account for low fat mass in myostatin deficient mice. Am J Physiol Endocrinol Metab 2011;300:1031–1037
43. Oldham JM, Osepchook CC, Jeanplong F, et al. The decrease in mature myostatin protein in male skeletal muscle is developmentally regulated by growth hormone. J Physiol 2009;587:669–677
44. Argilés JM, López-Soriano FJ, Busquets S. Therapeutic potential of interleukin-15: a myokine involved in muscle wasting and adiposity. Drug Discov Today 2009;14:208–213
45. Rasmussen MH. Obesity, growth hormone and weight loss. Mol Cell Endocrinol 2010;316:147–153
46. Rasmussen MH, Juul A, Kjems LL, Skakkebaek NE, Hilsted J. Lack of stimulation of 24-hour growth hormone release by hypocaloric diet in obesity. J Clin Endocrinol Metab 1995;80:796–801